[AMERICAN JOURNAL OF SCIENCE, VOL. 263, JUNE 1965, P. 512-536]

A PETROGENETIC GRID FOR THE FE-MG SILICATES OF PELITIC SCHISTS*

ARDEN L. ALBEE

Division of the Geological Sciences, California Institute of Technology
Pasadena, California

ABSTRACT. The topology of the reaction surfaces for the phases—garnet, chloritoid, staurolite, kyanite, cordierite, chlorite, and biotite—is shown for two limiting sections of P_s, T, P_{H_2O} space for the part of the system—SiO_2–Al_2O_3–FeO–MgO–K_2O–H_2O in which quartz and muscovite are stable. The basic assumption made is that the course of progressive metamorphism is primarily one of progressive dehydration with a progressive restriction of the fields of the most hydrous minerals, notably chlorite. The resulting petrogenetic grids for the surfaces $P_s \approx P_{H_2O}$ and $P_s \approx \frac{\rho_s}{\rho_{H_2O}} P_{H_2O}$ are predominantly theoretical and should serve as a useful check in assigning natural metamorphic sequences to their relative pressure-temperature relationships.

INTRODUCTION

As more detailed studies of regional metamorphic areas have appeared it has become apparent that the classical Dalradian sequence, chlorite–biotite–garnet–staurolite–kyanite–sillimanite, should not be considered the only normal sequence of progressive regional metamorphism. Read (1952) distinguished the Dalradian from the Buchan type of metamorphism, and Miyashiro (1958) distinguished the Dalradian and the central Abukuma types. In 1961 Miyashiro described five "metamorphic facies series" based on the inferred pressure-temperature relationships of observed natural sequences and upon correlation with experimental data, primarily on the relationships of kyanite–andalusite–sillimanite and jadeite + quartz-albite. Tröger (1963) has distinguished 12 different facies series, correlating them with different geothermal gradients.

The wide range of rock composition makes it necessary to define isograds in terms of the trace of a specific reaction surface upon the Earth's surface rather than upon the initial appearance of a phase in a rock of a fixed composition. Francis (1956) used specific reactions to define more precisely the facies boundaries in pelitic schists at the middle grades of metamorphism. Thompson (1955) outlined the thermodynamic basis for formulating a petrogenetic grid and in 1961 applied these ideas to a subsystem of the pelitic schist composition. He outlined the topology of univariant reactions for the system SiO_2–Al_2O_3–Na_2O–K_2O–H_2O in an arbitrary section of P_s, T, a_{H_2O} space.

The present paper is an attempt to show the topology of reaction surfaces in two limiting sections of P_s, T, P_{H_2O} space for a part of the system SiO_2–Al_2O_3–FeO–MgO–K_2O–H_2O. The basic assumption made is that the course of progressive metamorphism is primarily one of progressive dehydration with a progressive restriction of the fields of the most hydrous minerals, notably chlorite. The P-T slopes of the univariant curves are calculated following approximations suggested by Thompson (1955) and Fyfe, Turner, and Verhoogen (1958), and their relationships inferred from the theory of chemographic relations, ably summarized by Niggli (1954) and Korzhinskii (1959).

* Contribution No. 1277.

The resulting petrogenetic grids are predominantly theoretical and should serve as a useful check in assigning natural metamorphic sequences to their relative pressure-temperature relations.

COMPONENTS, PHASES, PHASE DIAGRAM, AND VARIABLES

Pelitic schists contain phases that to a first approximation lie in the system SiO_2–Al_2O_3–FeO–MgO–K_2O–H_2O, and quartz-bearing assemblages at a given P_s, T, and P_{H_2O}[1] may be shown graphically in a tetrahedron with the apices Al_2O_3–K_2O–FeO–MgO. With the further restriction that muscovite be present these assemblages may be projected into a plane—graphically a projection through muscovite to the Al_2O_3–FeO–MgO plane (Thompson, 1957). In accordance with the phase rule the 3-phase assemblages in such a diagram may contain one additional phase for each of several other components, such as Na_2O, CaO, Fe_2O_3, TiO_2, et cetera, in addition to quartz, muscovite, and, under certain conditions, fluid. Two-phase assemblages may contain two additional phases for one of these other components.

In this paper we shall be concerned with assemblages that meet these restrictions such that we can treat this projection as a true phase diagram showing the phases stable in this 3-component system in equilibrium with quartz and muscovite. We will further restrict ourselves to the consideration of only three variables—T, P_s, and P_{H_2O}—inasmuch as we will be concerned primarily with dehydration reactions. We shall consider the relations of quartz, muscovite, chlorite, biotite, garnet, chloritoid, staurolite, cordierite, and aluminum-silicate. Our primary concern is the topologic relationships between the Fe-Mg silicates, and the aluminum-silicates (kyanite, sillimanite, andalusite, mullite, pyrophyllite, and kaolinite) will be regarded initially as a single phase, kyanite. Figure 1a shows the positions of these phases on the pseudoternary phase diagram. The relative Fe/Mg contents of these phases are not completely known but for the purposes of this paper are assumed to be: (Fe/Mg): garnet > chloritoid > staurolite > biotite > cordierite > chlorite as based on data from (Albee, in press; Barker, 1962; Chinner, 1962; Green, 1963; Phinney, 1963; Snelling, 1957a,b; Thompson, 1957). Hence, the composition of all these phases will fall within the area between kyanite–garnet–biotite–chlorite. It is convenient to simplify the relations on the diagram further by treating the composition of chloritoid and staurolite as colinear between kyanite and garnet and of cordierite as colinear between kyanite and chlorite. Thus, the true reaction for the disappearance of chloritoid might be: chloritoid → staurolite + garnet + chlorite, but it will be simplified to the limiting equation: chloritoid → staurolite + garnet, inasmuch as the full equation requires a precise knowledge of the Fe/Mg in each phase for the exact conditions at the limit of chloritoid stability.

It is also convenient to simplify the topology of each diagram by limiting the compositional variation in the phases and restricting the 2-phase fields to

[1] P_{H_2O} as used here is $P_{E_{H_2O}}$, as defined by Greenwood (1961, p. 3924). It may vary from $P_{H_2O} = P_s$ in a fluid phase of pure H_2O at the same pressure as the solid phases to $P_{H_2O} = 0$ for a completely water-free system.

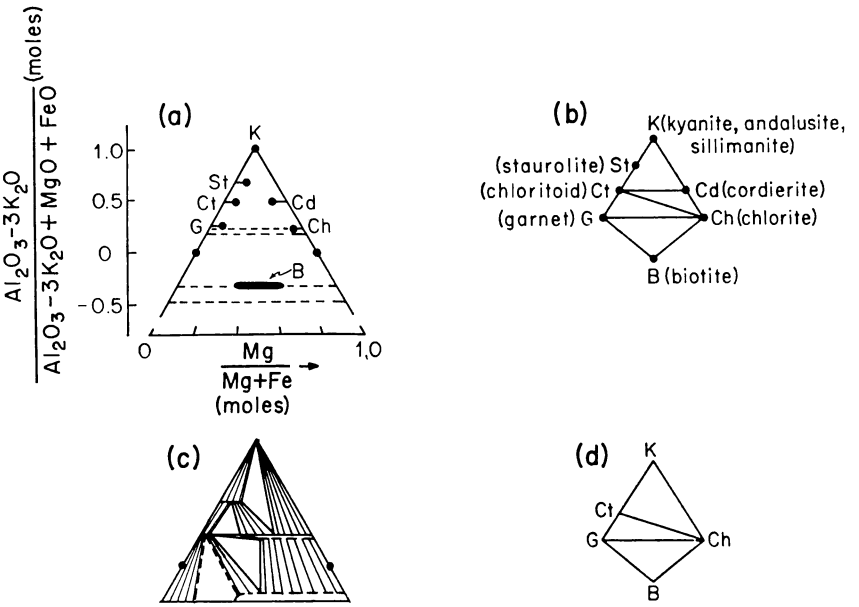

Fig. 1. System SiO_2–Al_2O_3–MgO–FeO–K_2O–H_2O showing possible phases in equilibrium with quartz and muscovite at P_s, T, P_{H_2O} (after Thompson, 1957):

a. circles indicate position of phases on the diagram with the assumed relative Fe/Mg,
b. schematic reduction of (a) which largely ignores Fe/Mg ratios of the phases,
c. typical facies type (Albee, in press),
d. schematic reduction of (c).

a line. However, the topology is preserved as seen in the examples in figure 1. Any such single topology as in figure 1c will be referred to as a "facies type" (Thompson, 1961).

Chlorite "disappears" at the biotite or garnet zone in many metamorphic terranes, yet experimental work indicates that magnesium-rich chlorite has a field of stability in rocks of the proper composition extending nearly to the maximum temperatures of metamorphism. Mg-chlorite is stable to 720°C at 2 kb P_{H_2O} (Yoder, 1952). The "disappearance" of chlorite is due to the restricted compositional range of pelitic schists within the diagram and to the gradual restriction of the stability field of chlorite within the diagram. In the diagrams to follow, chlorite is shown as stable to the highest temperature but with a high Mg/Fe and a restricted field of stability on the diagram.

In the general case of 5 or more phases in a 3-component system in P_s–T–P_{H_2O} space there are one or more univariant lines, each with 5 bivariant surfaces radiating from it. We can deduce the topology of the intersection of these lines and surfaces with a surface (not necessarily planar) that passes through the space in such a way as to intersect the common assemblages found in regionally metamorphosed rocks. It is convenient to choose a surface with a systematic relationship between P_s, P_{H_2O}, and T. For example, we might use

the surface $P_{H_2O} \approx P_s$, T corresponding to the usual conditions for hydrothermal experimental work. On this surface a typical metamorphic dehydration reaction would have a positive slope for $\frac{dP_s}{dT}$, becoming steeply positive at high P_s.

Thompson (1955) has shown that steeply negative slopes result from two likely relationships between P_s and P_{H_2O}: "fissure equilibrium" and nonisothermal steady state diffusion upward of H_2O. It is convenient to examine the topology of the trace of the reaction surfaces upon the $P_s \approx \frac{\rho_s}{\rho_{H_2O}} P_{H_2O}$, T surface, corresponding to the "fissure equilibrium" case.

PROCEDURE FOR CALCULATING THE SLOPES OF UNIVARIANT REACTION LINES

The slopes of the univariant reaction lines can be calculated for two sections through P_s–T–P_{H_2O} space using a series of approximations. In a typical dehydration reaction:

$$A_s + B_s \rightleftarrows C_s + D_s + n_{(H_2O)_f}$$

where the subscript s indicates solid phases and the subscript f indicates a fluid phase which is assumed to be pure H_2O. The slope is given by the relation (Thompson, 1955, p. 83):

$$\left(\frac{dP_s}{dT}\right)_{\Delta G=0} = \frac{\Delta S}{\Delta V_s + n_{H_2O} V_{H_2O}\left(-\frac{dP_{H_2O}}{dP_s}\right)}$$

where V_{H_2O} is the molar volume of water at specified P_{H_2O} and T, and n_{H_2O} is the number of moles of H_2O given off in the reaction.

Case I: $P_{H_2O} \approx P_s \approx 2.5$ *kb*; $T \approx 500°C$.—Case I assumes that the fluid phase consists of pure H_2O at the same pressure as the solid phases and corresponds to the usual conditions of hydrothermal experimental work if the small amount of dissolved impurities is neglected. In general large positive slopes are obtained.

TABLE 1

Mineral	Formula	Molar volume (25°C) (cc)	Source
staurolite (St)	$Fe_2Al_9Si_4O_{24}H$	223	Juurinen (1956)
kyanite (K)	Al_2SiO_5	44.2	Skinner, Clark, and Appleman (1961)
chloritoid (Ct)	$Fe(OH)_2Al_2SiO_5$	69.7	Halferdahl (1961)
garnet (G)	$Fe_3Al_2(SiO_4)_3$	115	Skinner (1956)
chlorite (Ch)	$Mg_5Al(AlSi_3O_{10})(OH)_8$	209	Shirozu (1958)
muscovite (Mu)	$KAl_2(AlSi_3O_{10})(OH)_2$	141	Yoder and Eugster (1955)
biotite (B)	$K(Mg, Fe)_3(AlSi_3O_{10})(OH)_2$	151	Wones (1963)
cordierite (Cd)	$Mg_2(Al_4Si_5O_{18})$	233	Schreyer and Schairer (1961)
quartz (Q)	SiO_2	22.7	

The molar volumes of the solid phases are given in table 1 along with the formulas used. It was assumed that $\left|\frac{\partial \Delta V_s}{\partial P}\right|_T$ and $\left|\frac{\partial \Delta V_s}{\partial T}\right|_P$ are zero or tend to cancel. V_{H_2O} was taken as 24.3 cc/mole at this temperature and pressure (Kennedy, 1950).

ΔS is small for reactions that do not involve dehydration or hydration and that do not involve a change in the first-order coordination numbers of cations with 4- or 6-fold coordination. The entropies of silicates can be approximated with reasonable accuracy by summing the entropies of the component oxides (Latimer, 1951; Fyfe, Turner, and Verhoogen, 1958, p. 26-27, 116). Hence, the entropy change in a dehydration reaction is approximately the entropy of the H_2O in the fluid phase minus the entropy of H_2O in the solid phase. The entropy of H_2O released in a dehydration reaction at 298°K was estimated as 9.4 cal/deg mole H_2O by Fyfe, Turner, and Verhoogen (1958, p. 117), a value close to the extrapolated value for ice at the same temperature. Fyfe also estimated the value for higher temperatures by a smooth extrapolation from 298°K to a value at 500°K, derived from the apparent entropy of H_2O in boehmite, and to a value at 600°K, derived from the apparent entropy of H_2O in brucite. The correctness of this extrapolation is supported by recent measured values of the increments in the apparent entropy of H_2O in muscovite from 400°K to 1000°K (Pankratz, 1964), based on measurements on both muscovite and dehydrated muscovite. The entropy of dehydrated muscovite at 298°K was not reported, but the entropy of muscovite at 298°K is 69.0 ± 0.7 cal/deg mole, and the summed entropy values of the oxides is 59.4 cal/deg mole, yielding an apparent entropy of H_2O in muscovite of 9.6 cal/deg mole at 298°K. With this supporting evidence the ΔS per mole of H_2O released in a dehydration reaction was taken from figure 33 of Fyfe, Turner, and Verhoogen (1958) as approximately 14 cal/deg mole (590 dj/deg mole) at $P_{H_2O} = 2.5$ kb and T = 500°C.

In several reactions considered in this paper, the first-order coordination of Al changes from six to four or from four to six. A further correction to the ΔS was made for these reactions, assigning a value to ΔS ($Al^{VI} \rightarrow Al^{IV}$) of +80 dj/deg mole Al. This value was based on the following data: albite $\rightleftarrows$ jadeite + quartz (83 dj), albite + nepheline $\rightleftarrows$ 2 jadeite (81 dj), and a calculated value of 76 dj/deg mole using the experimental slope of Clark (1961) in conjunction with the ΔV for the reaction, kyanite $\rightleftarrows$ sillimanite.

Case II: Osmotic equilibrium between rock and water-filled fissure for $P_s \approx 2.5$ kb, $T \approx 500$°C.—Thompson (1955, p. 89, 95) has shown that large negative slopes for P-T curves result from two possible natural relationships between P_s and P_{H_2O}: (a) osmotic equilibrium between rock and an H_2O-filled fissure extending to the surface, and (b) nonisothermal, steady-state upward diffusion of H_2O. The term $\left[n_{H_2O} V_{H_2O} \frac{dP_{H_2O}}{dP_s} \right]$, which is the fluid contribution to the volume change involved in the reaction, can be approximated for "fissure equilibrium" as follows:

$$dP_{H_2O} = \frac{\rho_{H_2O}}{\rho_s} dP_s = \frac{M_{H_2O}}{V_{H_2O}{}^m} \frac{1}{\rho_s{}^m} dP_s$$

$$\frac{dP_{H_2O}}{dP_s} = \frac{M_{H_2O}}{V_{H_2O}{}^m \rho_s{}^m} \approx \frac{6.7}{V_{H_2O}{}^m}$$

where M_{H_2O} and $V_{H_2O}{}^m$ are the molar weight (18 gs) and the average molar volume of water over the column, and $\rho_s{}^m$ ($\approx$ 2.7 g/cc) is the average density of the overlying rock column. Thompson (1955, p. 89) argues that the molar volume of H_2O at a certain point in the column is nearly equal to its mean value over the entire overlying column.
Thus:

$$V_{H_2O} \approx V_{H_2O}{}^m$$

and:

$$\left[n_{H_2O} V_{H_2O} \frac{dP_s}{dP_{H_2O}} \right] = n_{H_2O} V_{H_2O} \cdot \frac{6.7}{V_{H_2O}{}^m} = 6.7 \cdot n_{H_2O}$$

where 6.7 is interpreted as the "effective molar volume" of water under the conditions of "fissure equilibrium".

The following forms are convenient for calculation:

Case I:
$$\frac{dP_s}{dT} = \frac{\Delta S/n_{H_2O}}{\Delta V_s/n_{H_2O} + V_{H_2O}} = \frac{590^2}{(V_s/n_{H_2O}) + 24.3}$$

Case II:
$$\frac{dP_s}{dT} = \frac{\Delta S/n_{H_2O}}{\Delta V_s/n_{H_2O} + V_{H_2O} \frac{dP_s}{dP_{H_2O}}} = \frac{590^2}{(V_s/n_{H_2O} + 6.7}$$

We are mainly interested in the topology of the grid and hence the relative slopes of the lines, thus the error in the values assigned to ΔS and ΔV are insignificant to the extent that they are the same or proportional for all reactions. However, owing to the approximations and the nature of the equation there is greater uncertainty in the slope value for large slopes, since in such cases $\Delta V_s/n_{H_2O}$ approaches –24.3 or –6.7; in fact the sign may be wrong for very steep slopes. Small negative or positive slopes occur for many reactions that have cordierite as a reactant. The $\Delta S/n_{H_2O}$ is greatly decreased by the entropy change for $Al^{IV} \rightarrow Al^{VI}$, and $\Delta V_s/n_{H_2O}$ is large and negative. For such reactions the value of the slope is quite uncertain, but its sign is correct.

PROCEDURE FOR DERIVATION OF THE PETROGENETIC GRIDS

An invariant point for a 3-component system on such an arbitrary surface in P_s–T–P_{H_2O} space requires that five phases be in equilibrium. For the general case with seven phases taken five at a time there will be 21 invariant points, each with five univariant reaction lines radiating from it. However, each line will be common to three invariant points, either stable or metastable, so that there will be only 35, rather than 105, univariant reaction lines. Korzhinskii (1959, p. 125) has defined a 3-component system with two independent vari-

[2] The entropy correction for any coordination change of Al is not included.

ables[3] and seven phases as one with (–2) degrees of freedom and has outlined the technique of deriving the full topology of such a system. He demonstrates that the full system can be derived if the slopes of the 15 univariant lines associated with three invariant points are known, but that four variants result from different positions of the three initial invariant points. It is necessary to use natural assemblages to choose between these variants.

In this paper the choice was based upon the basic assumption of a progression from the most hydrous possible arrangements of these phases for the phase diagram to the least hydrous possible arrangement, culminating in the breakdown of muscovite and biotite. In particular the author had noted the importance of the univariant reaction, garnet + chlorite → chloritoid + biotite, in distinguishing a number of different metamorphic areas. The most hydrous, high temperature facies type known to the author is that from the Lincoln Mountain area, Vermont (Albee, in press), where chlorite and muscovite are stable with all other phases stable in the diagram (biotite, garnet, chloritoid, and kyanite) (see fig. 1). This facies type contrasts sharply with facies types where biotite and muscovite are stable with all the phases stable in the diagram (garnet, staurolite, kyanite or sillimanite, cordierite) (for example, Green, 1963). Even less hydrous are facies types where muscovite but not biotite is stable with all the phases stable in the diagram.

Initially, an approximation of the topology of the system was inferred by starting with the Lincoln Mountain facies type and moving away from it in steps of a single univariant dehydration reaction. The four possible steps are: the appearance of staurolite (chloritoid + kyanite → staurolite), the appearance of cordierite (kyanite + chlorite → cordierite), the disappearance of chloritoid (chloritoid → kyanite + garnet), and the transition (garnet + chlorite → chloritoid + biotite). At successively higher temperatures staurolite was assumed to appear, chloritoid to disappear, and staurolite to disappear. Cordierite was assumed to appear at lower pressure. The sequence of stable and metastable portions of the univariant lines around each table invariant point was analyzed using "Schreinemaker's rules" (see Niggli, 1954, p. 403-412 for an able summary). In the bundle at each invariant point the univariant lines were put in the proper sequence such that H_2O was given off on the high temperature side of the reaction.

Even without knowing the P-T slopes, the first three of the four possible steps suffice to define the topology of the 3-component system with six phases, K, St, Ct, G, Cd, Ch, shown in figure 2. Five of the invariant points are stable, and one is metastable. If none of the phases are colinear, an invariant point will involve five of the six phases and is designated on figure 2 by brackets [ ], which contain the abbreviation for the phase not involved. The point [Ch, Cd] actually consists of the coincidence of the two stable invariant points [Ch] and

[3] P_s, P_{H_2O}, and T are used as variables, but the surface is defined by a relationship between P_s and P_{H_2O} so that there are only two independent variables. The seven phases considered (K, St, Ct, G, B, Ch, Cd) must be described in terms of six components, but in the chemographic region where quartz plus muscovite occurs there are only three "critical" or "determining" components. An invariant point will actually have seven condensed phases, including quartz and muscovite, as well as a fluid phase if $P_{H_2O} = P_s$.

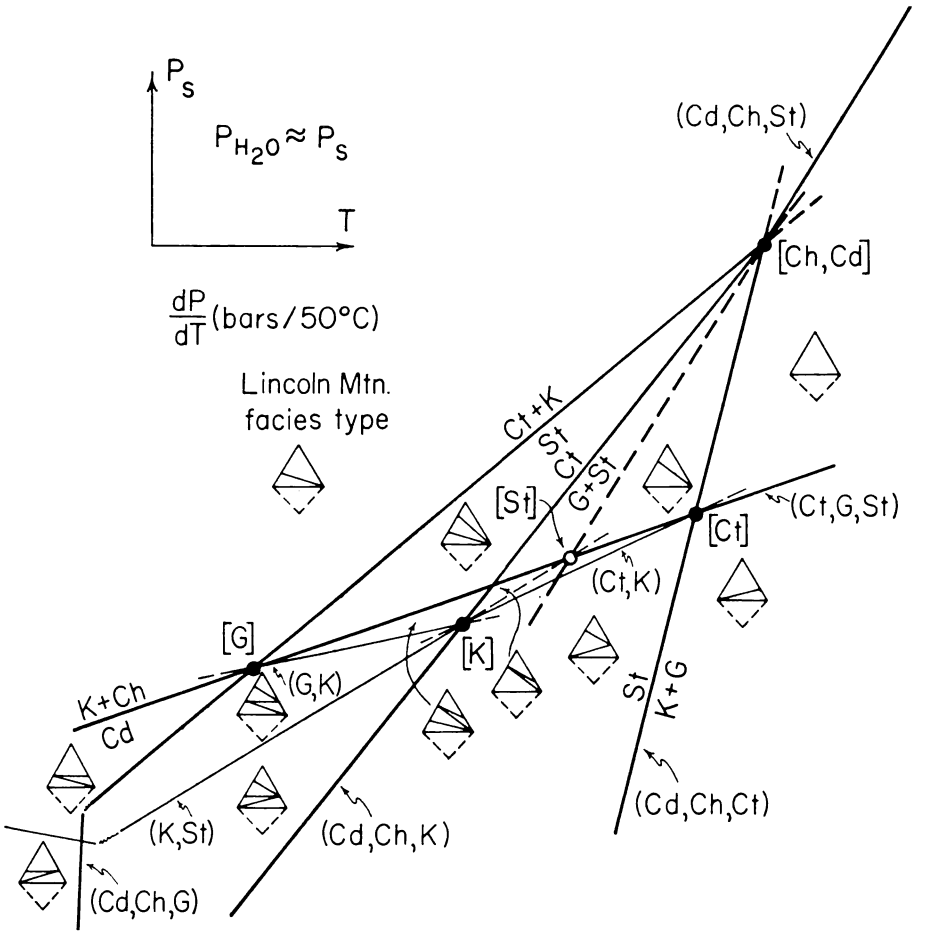

Fig. 2. Topology of the 3-component system with the six phases—kyanite, staurolite, chloritoid, garnet, cordierite, and chlorite—for $P_{H_2O} \approx P_s$ as projected to P_s-T surface.

[Cd], due to the colinearity of staurolite and chloritoid between kyanite and garnet. The univariant lines are designated by parentheses ( ), containing the two phases not involved in the reaction. Each univariant line passes through the two invariant points (stable or metastable) derived from the noted phases. Thus the line (Ct, K) passes through the invariant points [Ct] and [K]. The lines (Cd, Ch, St), (Cd, Ch, G), (Cd, Ch, K), (Cd, Ch, Ct), and (Ct, G, St) are degenerate due to the colinearities and pass through the three invariant points derived from the noted phases.

The grid of figure 2 retains the garnet-chlorite join throughout because no reactions involving biotite have been considered. If the fourth possible step, the univariant reaction (G + Ch → Ct + B) is added to figure 2 the reaction line will terminate in an invariant point on the line (Cd, Ch. K) or on the line (Cd, Ch, St). A series of reactions will be introduced which, with increasing

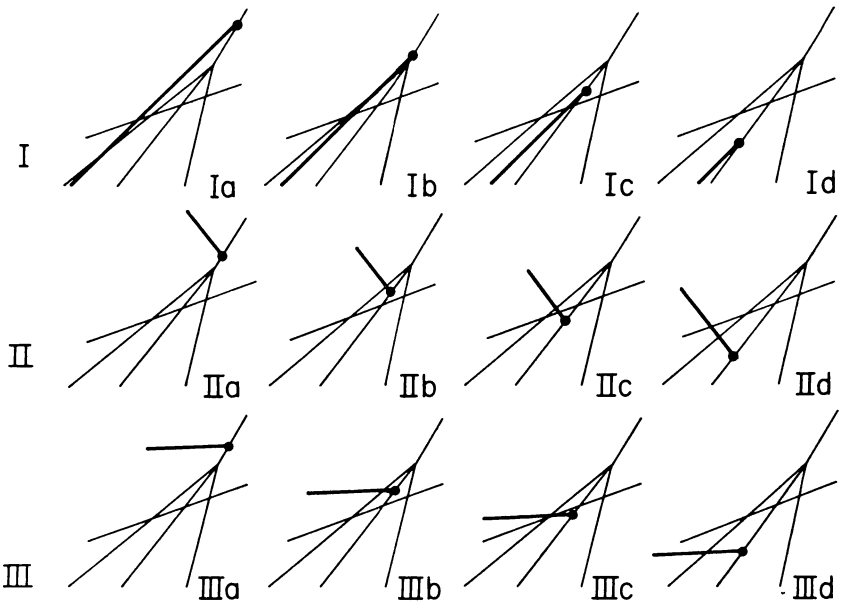

Fig. 3. Twelve variations resulting from different slopes of the reaction line (Cd, K, St) and different positions of the terminating invariant point relative to the topology of figure 2.

temperature, successively break joins to chlorite and replace them by joins to biotite. Figure 3 shows 12 different variants resulting from different slopes of this reaction line and different positions of this invariant point. When fully developed each of these 12 variants yield different topologies for the seven phase–3–component system. Each grid contains most of the commonly observed natural assemblages, making it difficult to decide which one corresponds most closely to the natural associations. The calculated slopes (table 2) of the lines (Cd, K, St), (B, Cd, Ch, G), and (B, Cd, Ch, K) indicate that row I of figure 3 corresponds to Case I for $P_{H_2O} \approx P_s$ and that row II corresponds to Case II for "fissure equilibrium".

Case Ic and IIb, both of which have the invariant point [K, Cd] in similar position, seem to correspond most closely to natural associations and sequences. This choice was based primarily upon the author's knowledge of chloritoid assemblages summarized in the following statements:

1. The composition of most quartz-muscovite schists lies below the garnet-chlorite join (Albee, 1952).

2. Chloritoid commonly does not appear in the transition from the garnet zone to the staurolite zone because the rock compositions lie below the garnet–chlorite join; thus staurolite first appears in the rock by the reaction garnet + chlorite → staurolite + biotite.

3. Chloritoid occurs most commonly in rocks with compositions lying above the garnet–chlorite join in the assemblages chloritoid–garnet–chlorite and chloritoid–chlorite, but the assemblage chloritoid–garnet–biotite occurs.

4. The transition garnet + chlorite → staurolite + biotite is more common in regionally metamorphosed rocks than the transition garnet + chlorite → chloritoid + biotite. However, both transitions do occur.

5. The assemblage chloritoid–garnet–biotite seems to occur both in areas where cordierite is present in rocks of different composition and in areas where cordierite is completely absent.

6. The assemblage chloritoid–cordierite–biotite is known in contact aureoles.

The reader may, however, develop the other cases using the calculated slopes given in table 2.

The slopes of all the univariant lines were calculated for balanced reactions with H_2O on the high temperature or product side of the equation. The formulas used for the minerals are given in table 1 and below. Quartz and muscovite were utilized as needed on either side of the equation. The slope of a univariant reaction line such as garnet + chlorite → cordierite + biotite is highly dependent upon the relative proportions of garnet and chlorite, due to the high H_2O content of chlorite, and upon the proportions of cordierite and biotite, due to the high gram atomic volume of cordierite. Hence it is necessary to specify the Mg/Fe in each of the four phases and to solve for the specific equation for each reaction line.

For the reaction lines about the invariant point [K, Cd] the following Fe and Mg contents were used:

Garnet	$Mg_{0.3}\,Fe_{2.7}\,Al_2\,(SiO_4)_3$
Chloritoid	$Mg_{0.2}\,Fe_{0.8}\,(OH)_2\,Al_2SiO_5$
Staurolite	$Mg_{0.5}\,Fe_{1.5}\,Al_9\,Si_4\,O_{24}\,H$
Biotite	$K\,Mg_{1.5}\,Fe_{1.5}\,(Al\,Si_3O_{10})\,(OH)_2$
Chlorite	$Mg_{2.6}\,Fe_{2.4}\,Al(Al\,Si_3O_{10})\,(OH)_8$

based on the data of Albee (in press), Green (1963), and Phinney (1963).

The colinearities make it unnecessary to specify the Fe and Mg content for the degenerate lines around the invariant point [B, Ch, Cd]. Calculations also indicated that a large departure from colinearity is necessary to change the calculated slopes of these lines significantly.

The Fe and Mg contents used in the higher temperature and pressure portion of the cordierite field near [Ct, Ch] were:

Garnet	$Mg_{0.7}\,Fe_{2.3}\,Al_2\,(SiO_4)_3$
Staurolite	$Mg_{0.6}\,Fe_{1.4}\,Al_9\,Si_4\,O_{24}\,H$
Biotite	$K\,Mg_{1.2}\,Fe_{1.8}\,(Al\,Si_3\,O_{10})\,(OH)_2$
Cordierite	$Mg_{1.2}\,Fe_{0.8}\,(Al_4Si_5O_{18})$

based on the data of Barker (1962), Best and Weiss (1964), and Chinner (1962). A less magnesium-rich cordierite composition ($Mg_{1.0}Fe_{1.0}$) was used in the lower pressure and temperature portion of the cordierite field following Chinner (1962).

Due to the colinearities the five degenerate lines include 17 of the 35 possible univariant reaction lines, and the topology of the grid and the correct slopes could be completely determined from the slopes of only 10 lines. Slopes were calculated for all the lines as a check and to permit the reader to construct other topologies. Table 2 gives the equation for the univariant reaction,

TABLE 2

Reactions and calculated slopes of univariant lines

Univariant Line	Reaction	$\Delta S/n_{H_2O}$ (dj/deg mole)	$\Delta V_s/n_{H_2O}$ (cc/mole)	$\frac{dP}{dT}$ (bar/deg) Case I $P_{H_2O} \approx P_s$	$\frac{dP}{dT}$ (bar/deg) Case II $P_{H_2O} \approx \frac{\rho_{H_2O}}{\rho_s} P_s$
[B, Cd, Ch, Ct]	6 St + 11 Q → 23 K + 4 G + 3 H_2O	590	–37.0	–19	–46
[B, Cd, Ch, G]	4 Ct + 5 K → 2 St + Q + 3 H_2O	590	–10.3	–160	+42
[B, Cd, Ch, K]	23 Ct + 8 Q → 4 St + 5 G + 21 H_2O	590	–15.1	–70	+64
[B, Cd, Ch, St]	3 Ct + 2 Q → 2 K + G + 3 H_2O	590	–17.0	–57	+80
[B, Ct, G, St]	8 K + 2 Ch + 11 Q → 5 Cd + 8 H_2O	770	+18.0	+31	+18
[B, Ct, K]*	208 St(0.6)** + 206 Ch(2.6) + 1481 Q → 152 G(0.3) + 495 Cd(1.2) + 928 H_2O	743	+10.5	+43	+21
[B, G, K]	24 St(0.5) + 15 Ch(2.6) + 114 Q → 35 Ct(0.2) + 44 Cd(1.0) + 37 H_2O	938	+43.7	+19	+14
[B, K, St]	25 Ct(0.2) + 3 Ch(2.6) + 39 Q → 6 G(0.3) + 11 Cd(1.0) + 12 H_2O	863	–0.2	+133	+36
[Cd, Ct, G]	6 St(0.5) + 30 Ch(2.6) + 54 Mu → 111 K + 54 B(1.5) + 3 Q + 123 H_2O	570	–17.0	–55	+78
[Cd, Ct, K]	95 G(0.3) + 324 Ch(2.6) + 499 Mu → 204 St(0.6) + 499 B(1.5) + 441 Q + 1194 H_2O	568	–15.2	–67	+62
[Cd, Ct, St]	3 G(0.7) + 24 Ch(2.6) + 43 Mu → 70 K + 43 B(1.5) + 11 Q + 96 H_2O	570	–16.5	–58	+77
[Cd, G, K]	285 Ct(0.2) + 183 Ch(2.6) + 278 Mu → 168 St(0.6) + 278 B(1.5) + 162 Q + 933 H_2O	574	–15.2	–68	+63
[Cd, G, St]	3 Ct(0.2) + 9 Ch(2.6) + 16 Mu → 28 K + 16 B(1.5) + 2 Q + 36 H_2O	570	–18.0	–50	+90
[Cd, K, St]	14 G(0.3) + 15 Ch(2.6) + 22 Mu → 51 Ct(0.2) + 22 B(1.5) + 36 Q + 9 H_2O	457	–17.0	–44	+63
[Ch, Ct, G]	2 St(0.6) + Cd(1.2) + 2 Mu → 13 K + 2 B(1.2) + H_2O	270	–84.4	–3.5	–4.5

TABLE 2 (Continued)

Univariant Line	Reaction	$\Delta S/n_{H_2O}$ (dj/deg mole)	$\Delta V_s/n_{H_2O}$ (cc/mole)	$\frac{dP}{dT}$ (bar/deg) Case I $P_{H_2O} \approx P_s$	$\frac{dP}{dT}$ (bar/deg) Case II $P_{H_2O} \approx \frac{\rho_{H_2O}}{\rho_s} P_s$
[Ch, Ct, K]	128 St(0.6) + 158 B(1.2) + 611 Q → 156 G(0.7) + 131 Cd(1.2) + 158 Mu + 64 H_2O	1245	+69.7	+16	+13
[Ch, Ct, St]	64 K + 22 B(1.2) + 47 Q → 12 G(0.7) + 15 Cd(1.2) + 22 Mu	4800	+759	+6.3‡	+6.3‡
[Ch, G, K]	80 Ct(0.2) + 53 Cd(1.0) + 30 Mu → 48 St(0.5) + 30 B(1.5) + 153 Q + 56 H_2O	287	-61.6	-5.2	-7.7
[Ch, G, St]	6 Ct(0.2) + 9 Cd(1.2) + 8 Mu → 32 K + 8 B(1.5) + 19 Q + 6 H_2O	110	-98.1	-1.2	-1.5
[Ch, K, St]	16 Ct(0.2) + 2 B(1.5) + 21 Q → 4 G(0.3) + 5 Cd(1.0) + 2 Mu + 16 H_2O	690	-2.3	+157	+31
[Ct, G, K]	16 St(0.6) + 14 Ch(3.0) + 119 Q + 4 Mu → 45 Cd(1.0) + 4 B(1.6) + 64 H_2O	798	+20.8	+29	+18
[Ct, K, St]	4 G(0.3) + 48 Ch(2.6) + 50 Mu + 99 Q → 51 Cd(1.0) + 50 B(1.5) + 192 H_2O	655	-1.8	+135	+25
[G, K, St]	2 Ct(0.2) + 6 Ch(2.6) + 15 Q + 6 Mu → 2 Cd(1.0) + 6 B(1.5) + 26 H_2O	658	-1.7	+132	+29

* Invariant points are listed alphabetically

** Mg content in the formula given in table 1

‡ No H_2O loss

$\Delta S/_{n_{H_2O}}$, $\Delta V_{s/n_{H_2O}}$ and the calculated slopes of the univariant reaction lines for both cases.

The original rough grids were adjusted using the calculated slopes. Although the univariant lines must be somewhat curved, straight lines were used[4] so that all 21 invariant points could be located and the correctness of the topology assured. The calculated slope for the reaction (St → K + G) does not fit the grid determined by the other lines(and its slope is strongly dependent upon the amount of H in staurolite. However, the H content of staurolite and its correct formula are, in fact, unknown (see discussion in Deer, Howie, and Zussman, 1963, v. 1, p. 153). The slope of this line on the grid is not its calculated slope but was fixed by the rest of the grid. A similar slope could be calculated if nearly twice as much H was assumed in the staurolite formula, corresponding to the suggestion of Deer, Howie, and Zussman. It should also be noted that if twice as much H is assumed in the staurolite formula, the calculated slopes for the reaction lines (B, Cd, Ch, G), (B, Cd, Ch, K), and (Cd, K, St) indicate that case IIIb of figure 3 is the correct topology for $P_s \approx P_{H_2O}$.

DISCUSSION OF THE GRIDS

Figure 4, A and B, shows the topology of the facies types on the $P_{H_2O} \approx P_s$-T surface as projected to a P_s-T surface (case I). Figure 5, A and B, shows the topology of facies types on the surface $P_{H_2O} \approx \frac{\rho_s}{\rho_{H_2O}} P_s$ as projected to a P_s-T surface (case II). Each grid holds to the basic premise of progressively less-hydrous facies types with increasing temperature, but the two grids have different topologies.

If none of the phases are colinear in multi-component space an invariant point will involve five of the seven phases and is designated on the diagrams by brackets [ ], which contain abbreviations for the two phases not involved. Similarly the univariant lines are designated by parentheses ( ). containing the three phases not involved in the reaction. For example, the invariant point [St, K] in the lower part of figure 4, A and B, is the locus of intersection for the univariant curves:

(Cd, K, St)	G + Ch → Ct + B
(G, K, St)	Ct + Ch → Cd + B
(Ch, K, St)	Ct + B → G + Cd
(B, K, St)	Ct + Ch → G + Cd
(Ctd, K, St)	G + Ch → Cd + B

Each univariant line, including both stable and metastable portions, passes through the three invariant points (stable or metastable) derived from the combinations of the noted phases. Thus the line (Cd, K, St) passes through the invariant points [Cd, St], [Cd, K], and [St. K].

Twelve of the 21 invariant points are stable in figure 4, and 11 are stable in figure 5. There appear to be two less on each grid because the point [B, Cd,

[4] The lines would be nearly straight above 4 kb if a lnP-T plot were used (see Kennedy, 1959).

Ch] in the upper portion of the diagrams actually consists of the coincidence of three stable invariant points, [B, Ch], [B, Cd], [Ch, Cd], due to the colinearities of staurolite and chloritoid between kyanite and garnet. The lines (B, Cd, Ch, K), (B, Cd, Ch, G), (B, Cd, Ch, St), and (B, Cd, Ch, Ct), which pass through this point, are degenerate, and their reactions only involve three phases. Such a line, (B, Cd, Ch, Ct), includes four lines, (B, Cd, Ct), (Cd, Ch, Ct), (B, Ch, Ct), and (B, Cd, Ch), and may include stable segments of all four.

The calculated P-T slopes yield the proper sequence around the invariant points with the exception of several lines whose slopes differ only within the error of the calculations. The line (Ch, Ct, St) is not a dehydration reaction and must have the same slope on both grids. The slope shown, which conforms to the rest of the grid, was calculated using the ΔS for the change in Al-coordination due to the participation of cordierite and chlorite in the reaction.

The exact value of the slopes in the two grids is not important. They are simply calculated for two limiting values of P_{H_2O} at $P_s \approx 2.5$ kb and $T \approx 500°C$ because the ΔS of dehydration and the molar volume of H_2O can be reasonably estimated under these conditions. The molar volumes and Al-coordination are different for kyanite, andalusite, and sillimanite, but those of kyanite were used through the calculations. The univariant reactions that involve an aluminum-silicate will have a break in slope at the transition from one aluminum-silicate to another. It seems preferable to extrapolate the topology of the grids to greater pressure than to attempt to estimate the ΔS of dehydration and the molar volume of water at greater pressure. An inspection of experimental dehydration curves of silicates at $P_{H_2O} \approx P_s$ shows that most of the curvature occurs below 2.5 kb and that the topology should be correct at much greater pressure. From this point on we shall discuss the grids in terms of pressures ranging from approximately 2.5-20 kb, a range in which the lines will be nearly straight.

The two different grids shown in figures 4 and 5 represent sections through P_s–T–P_{H_2O} space, and there must be a continuous transition from one to the other. This transition occurs in a series of topologies in which the lines (Cd, K, St), (Cd, Ct, K), and (Ct, K, St) successively have the same slope as and coincide with the line (B, Cd, Ch, K). These are the particular sections in which the disappearance of chloritoid coincides with the various reactions breaking the garnet-chlorite join. The four lines have similar slopes, and in some particular section the line (B, Cd, Ch, K) for the reaction (Ct $\rightarrow$ St + G) will *nearly* coincide with all the lines for the reactions: (G + Ch $\rightarrow$ St + B), (G + Ch $\rightarrow$ Ct + B), and (G + Ch $\rightarrow$ Cd + B). Figure 6 shows this situation, assuming that it occurs for P_{H_2O} approximately midway between P_s and $\frac{\rho_{H_2O}}{\rho_s} P_s$.

In figure 6 a number of univariant reactions coincide, and a large number of invariant points coincide. The coincidence of invariant points stable in either figure 4 or 5 is noted on the diagram. The grid is considerably simpler than those of figures 4 and 5, and a number of facies types and reactions are absent, being replaced by the double step (Ct $\rightarrow$ St + G) and (G + Ch $\rightarrow$

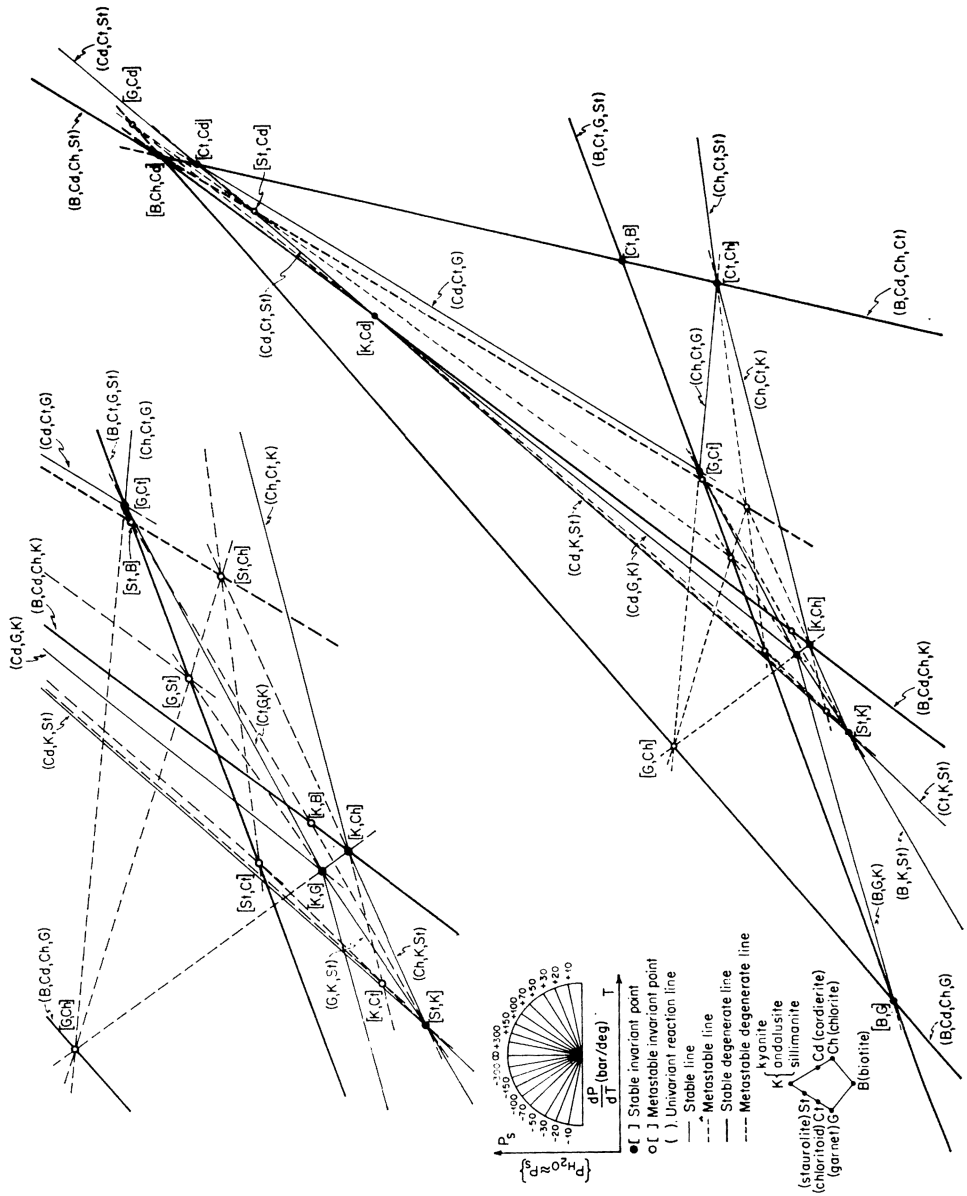

Fig. 4. Petrogenetic grid for Fe-Mg silicates of pelitic schists for $P_{H_2O} \approx P_s$ as projected to P_s-T surface. Figure 4A (left page) shows all univariant reaction lines and

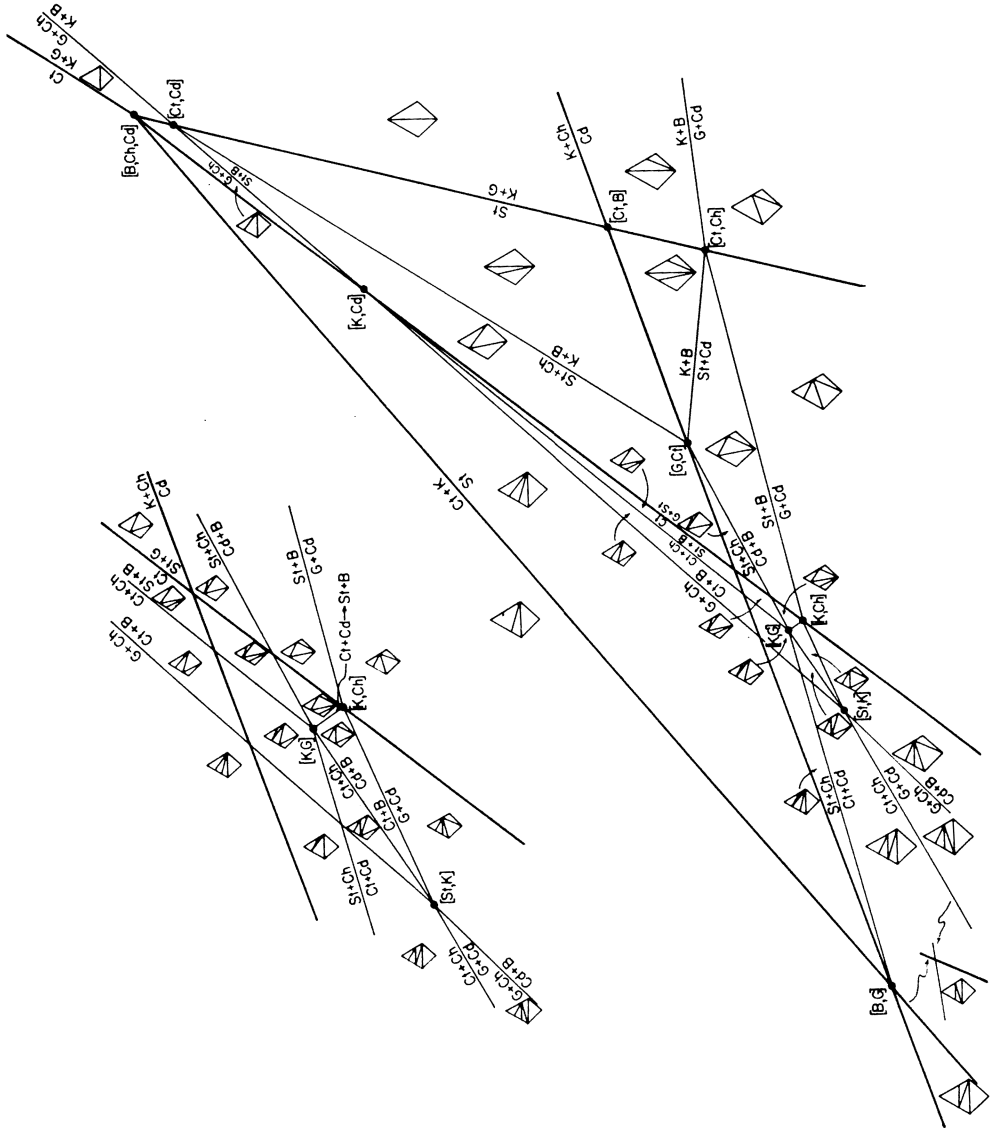

invariant points, both stable and metastable. Figure 4B (right page) shows the facies types and the simplified reactions for the stable univariant reaction lines.

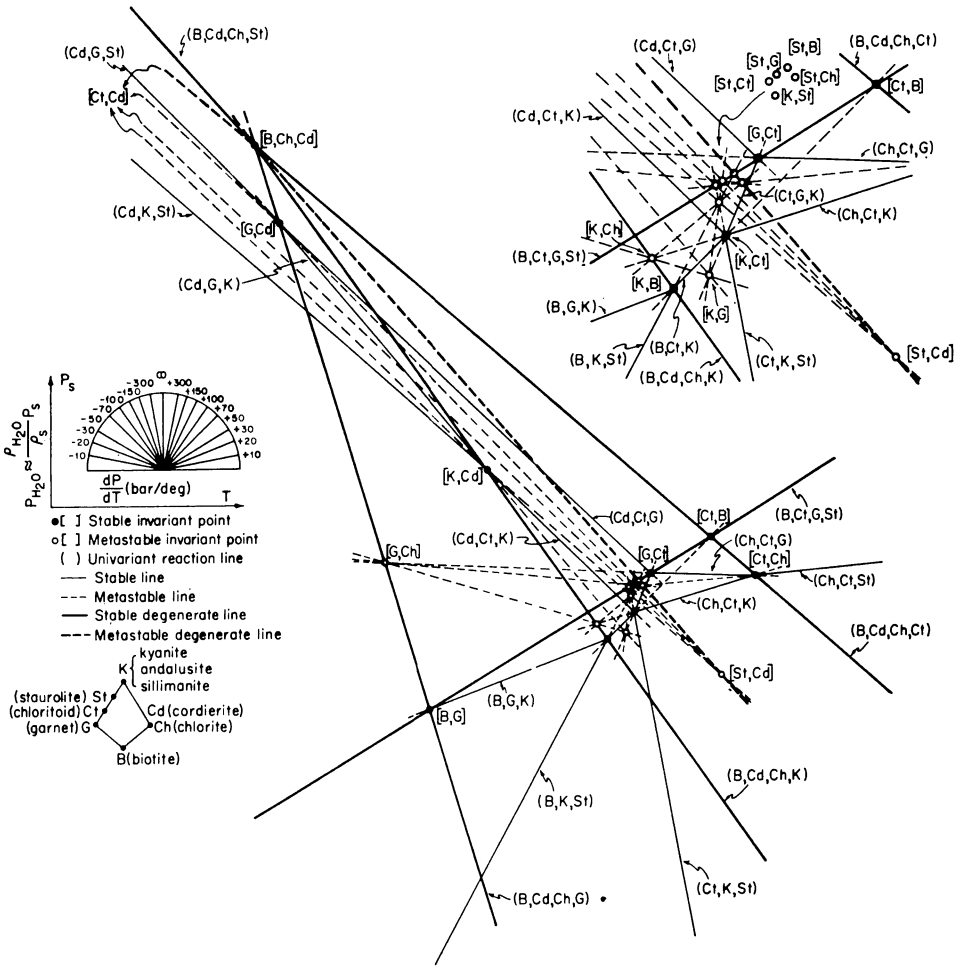

Fig. 5. Petrogenetic grid for Fe-Mg silicates of pelitic schists for $P_{H_2O} \approx \frac{\rho_{H_2O}}{\rho_s}$ P_s as projected to P_s-T surface. Figure 5A (left page) shows all univariant reaction lines

St + B) in the upper part of the diagram and by the double step (Ct → St + G) and (G + Ch → Cd + B) in the lower part. This situation may be commonly approached naturally as such a double step helps explain the rarity of stable staurolite–chloritoid assemblages. In fact, the calculated slopes of the critical univariant reaction lines are identical within the calculation errors for $P_s \approx P_{H_2O}$ (see table 2), and the slope differences have been exaggerated in figure 4. However, the assemblage chloritoid–cordierite–biotite and the occurrence of the assemblage garnet–chloritoid–biotite in areas with cordierite and

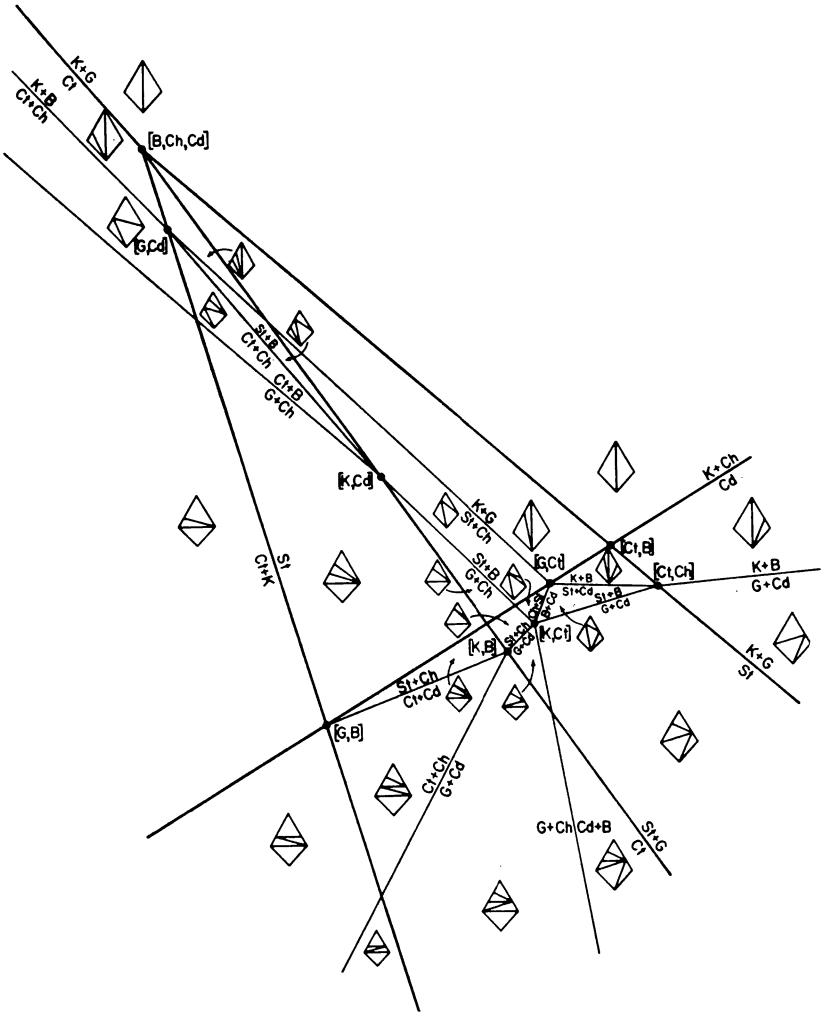

and invariant points, both stable and metastable. Figure 5B (right page) shows the facies types and the simplified reactions for the stable univariant reaction lines.

andalusite are both prohibited by the topologies of figures 5 and 6, indicating that the topology of figure 4 does occur in nature. The topology of figure 6 is probably approached for P_{H_2O} somewhat less than P_s, which may be a common set of natural conditions, especially for regional metamorphism. Hence, the simplified grid of figure 6 may describe many metamorphic areas.

The three grids shown will be limited on both the high and low temperature sides by other reactions and portions of the grid may become metastable, but most of the facies types shown on the grids have been described from

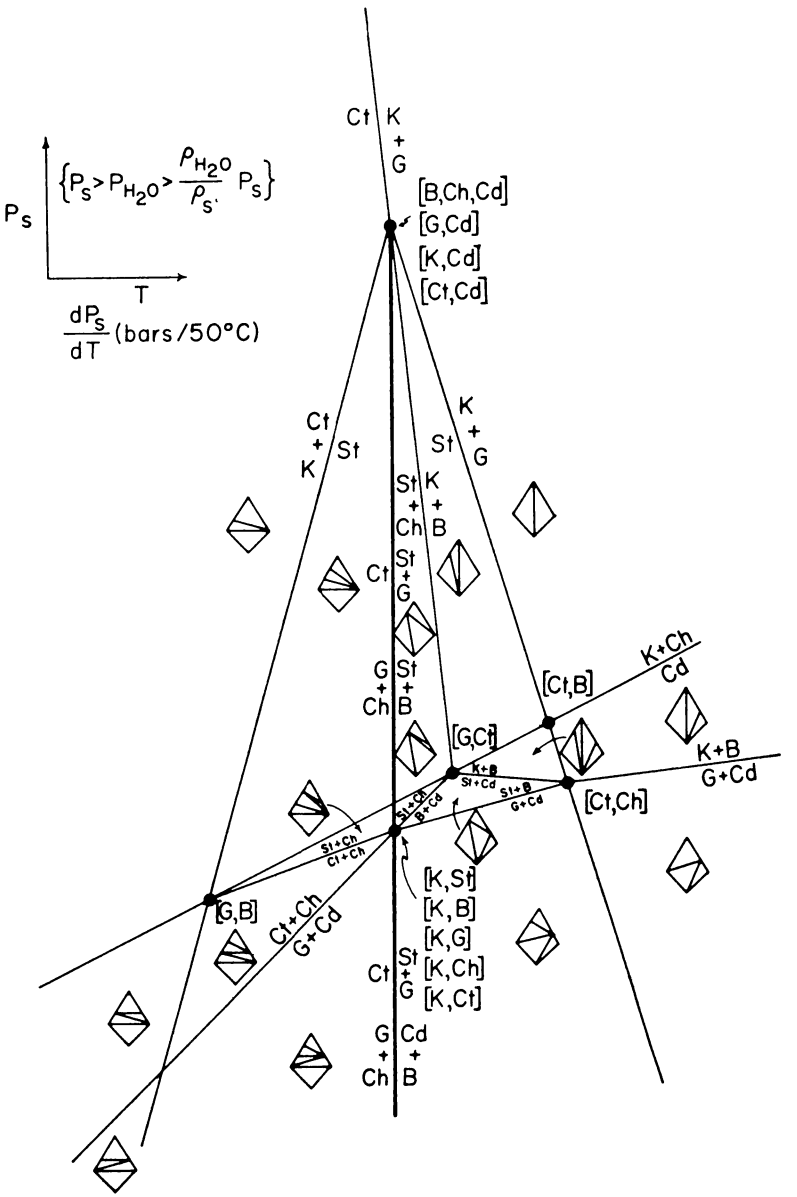
Ps
T
$\{P_s > P_{H_2O} > \frac{\rho_{H_2O}}{\rho_s} P_s\}$
$\frac{dP_s}{dT}$ (bars/50°C)
Ct K + G
[B,Ch,Cd]
[G,Cd]
[K,Cd]
[Ct,Cd]
Ct + K St
St K + G
St K + Ch B
Ct St + G
G St + Ch B
[Ct,B]
K+Ch Cd
[G,Ct]
K+B G+Cd
[Ct,Ch]
St+Ch Ct+Ch
St+Cd G+Cd
St+B G+Cd
K+B St+Cd
[K,St]
[K,B]
[K,G]
[K,Ch]
[K,Ct]
[G,B]
Ct+Ch G+Cd
Ct St + G
G Cd + Ch B

various localities and appear to be stable under natural conditions. On the high temperature side the grid will be terminated by successive reactions such as:

1. muscovite + quartz → $\left\{\begin{array}{l}\text{sillimanite}\\ \text{kyanite}\\ \text{andalusite}\end{array}\right\}$ + K-feldspar + H_2O
2. biotite + quartz → anthophyllite + K-feldspar + H_2O
3. biotite + quartz → hypersthene + K-feldspar + H_2O

These reactions do not seriously alter the topology of the individual facies types inasmuch as anthophyllite or hypersthene can replace biotite topologically and K-feldspar can replace muscovite. Additional invariant points will be introduced as the transitions occur, however, because the phases have a range in composition and will coexist over some temperature interval.

On the low temperature side the grids will be terminated by successive reactions such as:

1. pyrophyllite → (kyanite, andalusite, sillimanite) + quartz + H_2O
2. pyrophyllite + magnesium chlorite → cordierite + quartz + H_2O
3. chlorite + quartz → garnet + H_2O or
   chlorite + muscovite + quartz → garnet + biotite + H_2O
4. iron chlorite + pyrophyllite → chloritoid + quartz + H_2O
5. K-feldspar + chlorite → muscovite + biotite + quartz + H_2O
6. kaolinite + quartz → pyrophyllite + H_2O

The first of these reactions almost certainly overlaps part of the grid and makes part of it metastable, but the topology of the facies types is unchanged by either the first or the last reaction. All of the above reactions correspond to the basic premise of successively more hydrated facies types with decreasing temperature.

POSITION OF THE GRIDS IN P_s–T–P_{H_2O} SPACE

Experimental data is required to fix the position of the grids in P_s–T–P_{H_2O} space. The grids assume the coexistence of quartz plus muscovite plus anhydrous Al-silicate. and such natural assemblages do include the facies types for the highest and lowest temperatures at the intermediate pressure portion of the grids. The coexistence of quartz plus muscovite plus anhydrous Al-silicate is limited on the low and high temperature sides respectively by the reactions:

pyrophyllite → Al-silicate + quartz + H_2O

muscovite + quartz → Al-silicate + K-feldspar + H_2O

The position of the pyrophyllite breakdown curve is still quite uncertain despite the experimental work of Roy and Osborn (1954), Kennedy (1959)[5], Aramaki and Roy (1963), and Schreyer and Yoder (1964). The investigations of Yoder and Eugster (1954) and of Segnit and Kennedy (1961) on the

[5] Kennedy (personal communication, 1964) states that the temperatures given in his paper are now known to be much too high.

← Fig. 6. Petrogenetic grid for Fe-Mg silicates of pelitic schists in the range $P_s > P_{H_2O} > \frac{\rho_{H_2O}}{\rho_s} P_s$ as projected to P_s-T surface. The grid is for the particular section in which the heavy vertical line represents a coincidence of the reaction lines for the disappearance of chloritoid and the breaking of the garnet-chlorite join.

muscovite plus quartz breakdown curve are in substantial agreement, but above $P_s \approx P_{H_2O} \approx 5$ kb the curve is disrupted by melting phenomena. Using the approximations discussed earlier the calculated slopes at $P_s \approx P_{H_2O} \approx 2.5$ kb and $T \approx 500°C$ for both curves are close to 50 bar/deg. In comparison the experimentally-determined slope for muscovite plus quartz is about 45 bar/deg at $P_s \approx P_{H_2O} \approx 2.5$ kb and $T \approx 710°C$. The slope should be nearly the same for both curves, and the temperature interval between the curves should remain nearly constant despite change in P_s and P_{H_2O}. Extrapolation[6] of the data of Schreyer and Yoder (1964) for prophyllite suggests that this temperature interval is about 200°C and that the pyrophyllite breakdown curve is at about 510°C at $P_s \approx P_{H_2O} \approx 2.5$ kb and at about 590°C at $P_s \approx P_{H_2O} \approx 10$ kb. The muscovite plus quartz breakdown curve is at about 710°C at $P_s \approx P_{H_2O} \approx 2.5$ kb. Using the relationship of Greenwood (1961, p. 3925):

$$\left|\frac{\partial P_s}{\partial T}\right|_{P_{H_2O}} = \left[\frac{dP_s}{dT}\right]\left[\frac{\Delta V_s + \left[V_{H_2O}\right] P_{H_2O}}{\Delta V_s}\right]$$

where $\frac{dP_s}{dT}$ and ΔV_{H_2O} are evaluated for $P_{H_2O} = P_s$, the transition temperatures for the two reactions are about 390°C and 590°C respectively for $P_s = 8$ kb and $P_{H_2O} = 2.5$ kb, which corresponds approximately to the conditions of "fissure equilibrium".

Further temperature restrictions are imposed within this temperature interval by experimental work on two of the univariant reaction lines. The reaction for the P-T curve (B, Cd, Ch, K) is:

chloritoid + quartz → staurolite + garnet + H_2O

which corresponds to the experimentally-determined, quartz-deficient reaction (Halferdahl, 1961, p. 99):

Fe–chloritoid → Fe–staurolite + Fe–garnet + Fe–spinel + H_2O

At $P_{H_2O} \approx P_s \approx 10$ kb the reaction temperature is 700°C, and the slope is about +400 bar/deg. The curve (B, Cd, Ch, K) must lie at a somewhat lower temperature than the experimental curve; it has a calculated slope of +64 bar/deg for $P_{H_2O} \approx P_s \approx 2.5$ kb and $T \approx 500°C$. Lower pressure data are not available because under the experimental conditions at $P_{H_2O} \approx P_s \approx 6$ kb chloritoid goes to Fe–cordierite + Fe–spinel + H_2O.

---

[6] In these extrapolations use was made of Kennedy's (1959, p. 569) observation that at pressures greater than 4 kb (actually greater than 1-2 kb) plots of ln P versus T for dehydration reactions are nearly linear. This same observation provides a useful way to evaluate $\frac{dP}{dT}$ for some particular value of $P_s = P_{H_2O}$ from the small graphs which are usually published. Noting that for $P_{H_2O} = P_s >$ 1-2 kb dehydration curves are of the form:

$$\ln P = A + B\,T$$

then: $\frac{dP}{dT} = B\,P$ and $\frac{d \ln P}{dT} = B$

therefore: $\left[\frac{dP_s}{dT}\right]_{(P_s = P_{H_2O} = 2.5\text{ kb})} = \left[\frac{d \ln P}{dT}\right] \cdot 2.5$ kb

and $\frac{d \ln P}{dT}$ can be evaluated from a ln P, T plot.

The reaction for the line (B, Ctd, G, St) is: Al–silicate + chlorite + quartz → cordierite + H_2O. Schreyer and Yoder (1964, p. 293) have fixed this transition for magnesium cordierite at 685°C for $P_{H_2O} \approx P_s \approx 10$ kb and infer that it has a relatively small positive slope (shown as about +50 bar/deg on their diagram). The calculated slope is +18 bar/deg for $P_{H_2O} \approx P_s \approx 2.5$ kb and $T \approx 500$°C. This line (B, Ctd, St) is terminated on the low temperature end by the reaction:

pyrophyllite + Mg–chlorite + Al–silicate → Mg–cordierite + H_2O

at about 550°C and $P_{H_2O} \approx P_s \approx 5.0$ kb. They indicate (p. 302) that this intersection is within the stability field of sillimanite.

It would be valuable to superimpose the stability fields for the anhydrous Al-silicates upon these petrogenetic grids because their stability is independent of P_{H_2O}. The triple point is at 300°C and 8 kb according to Bell (1963) but has been placed at about 390°C and 8 kb by Khitarov and others (1963). There is some doubt as to whether the triple point is ever stable naturally. Assuming the experimental data are correct, it may be unstable even under the conditions of "fissure equilibrium". As noted above, the breakdown temperature for pyrophyllite at $P_s \approx 8$ kb and $P_{H_2O} \approx 2.5$ kb is about 390°C, well above the triple point temperature of Bell but close to that of Khitarov and others.

The slope of the kyanite–sillimanite transition is about +13.2 bar/deg (Clark, 1961), somewhat less than the slope of the line (B, Ct, G, St) which marks the first appearance of cordierite. The undoubted stable occurrence of kyanite with cordierite is rare, and the experimental work confirms that the kyanite–sillimanite transition is at a higher pressure, sub-parallel to (B, Ct, G, St). The calculated slope of the andalusite–sillimanite transition is about –17.7 bar/deg (Skinner, Clark, and Appleman, 1961, p. 666).

This experimental data is insufficient to fix the position of the grids in P-T space, in part due to experimental uncertainties such as the position of the pyrophyllite breakdown curve and in part due to apparent discrepancies with natural assemblages. For example, the experimental data (see Schreyer and Yoder, 1964, p. 303, fig. 5; and Segnit and Kennedy, 1961) suggest that the breakdown of muscovite plus quartz to Al-silicate plus K-feldspar always occurs within the stability fields of cordierite and sillimanite. However, the facies types above and below the line (Ch, Ct, St) on the right side of the grids occur commonly with either andalusite or sillimanite and with either muscovite or K-feldspar (Fyfe, Turner, and Verhoogan, 1958, p. 205-213; Read, 1952; Chinner, 1962; Best and Weiss, 1964). These natural assemblages suggest that the andalusite–sillimanite transition and the muscovite breakdown intersect the line (Ch, Ct, St) in this region, but this is prohibited by the experimental data described above.

A further restriction on the position of the grid is provided by a detailed study (Albee, in press) of the facies type that lies to the left of the (Cd, St, K) line on the grids and contains the assemblage kyanite–chloritoid–chlorite. The coexistence of kyanite plus muscovite plus quartz and comparison of the composition of coexistent muscovite and paragonite and of O^{18}/O^{16} ratios for co-

existent quartz and magnetite with experimental values indicate that this facies type in the Lincoln Mountain area formed at $P_s \approx 11$ kb, $T \approx 550°C$, and P_{H_2O} enough less than P_s, to depress the pyrophyllite breakdown temperature by at least 40°C.

Most of the grid should be stable over the range from $P_{H_2O} \approx P_s$ to $P_{H_2O} \approx \frac{\rho_{H_2O}}{\rho_s} P_s$, but the higher pressure portion may be made metastable by the bounding reactions at both extremes. The grid will have a temperature interval of about 200°C, but the temperature for any given reaction, including the bounding reactions, changes greatly with both P_s and P_{H_2O}.

CORRELATION OF THE GRIDS WITH OBSERVED FACIES SERIES

It is difficult to assign a definite order through the grid for any particular metamorphic area because of the lack of detailed descriptions of assemblages. The association of chloritoid plus staurolite and of chlorite plus staurolite or kyanite or even garnet is commonly, almost automatically, rejected as a disequilibrium occurrence, but such assemblages are essential to the definition of a path through the grids. To assign a definite order it is also virtually necessary to know the assemblages in rocks whose composition lies above the garnet–chlorite join, rocks more aluminous than most pelitic rocks.

The typical Dalradian, Barrovian, or kyanite–sillimanite facies series (Miyashiro, 1961), which is characterized by the presence of staurolite, kyanite, and sillimanite and the absence of cordierite, probably passes between the invariant point [K, Cd] and the line (B, Ctd, G, St) inasmuch as staurolite–garnet–chlorite assemblages seem relatively rare. The typical central Abukuma or andalusite–sillimanite facies series (Miyashiro, 1961) is characterized by the occurrence of cordierite, andalusite, and sillimanite and the absence of staurolite and kyanite. It, as well as many contact metamorphic facies series, would lie below the invariant points [K, Ch] and [Ct, Ch] on figure 4 or [K, B], [K, Ct], and [Ct, Ch] on figure 5. The typical Buchan or low-pressure intermediate facies series (Miyashiro, 1961) is characterized by the occurrence of corderite, staurolite, andalusite, and sillimanite and the absence of kyanite. It lies below the kyanite–sillimanite transition, predominantly below the line (B, Ctd, G, St) and above the same series of invariant points.

It might be thought that a calculated "normal" geothermal gradient might serve as a guide to the path through the grids. However, as pointed out by Fyfe and Verhoogen (Fyfe, Turner, and Verhoogan, 1958, p. 196) high grade metamorphism occurs only under conditions of greatly increased heat flow. In particular, no "reasonable" calculated geothermal gradient would cross the kyanite → sillimanite transition with increasing pressure and temperature although the transition kyanite → sillimanite is common in metamorphic terranes. It seems evident that the kyanite → sillimanite transition occurs only when there is a perturbation on the "normal geothermal gradient" such as might be related to intrusive rocks on a local scale or to disturbances in the mantle in regional occurrences.

CONCLUSION

It should be emphasized that despite the apparent complexity of these grids they represent a gross simplification of the natural assemblages. The compositions of many graywackes is such that muscovite disappears at a rather low grade, and hence these rocks are not represented. Possible reactions involving Fe–oxides have not been used, and no consideration has been given to a_{O_2} or a_{CO_2} as variables. The complication of the presence of additional phases stabilized by Mn, Ca, Na, et cetera has not been treated. No attention has been paid to the problem of describing equilibrium assemblages in spite of partial retrogradation. So, to this extent, the grids represent an idealization of what should occur if nature were well behaved.

It is believed that the grids should:

1. Help to assign facies series and facies types to their relative P, T relationships,

2. Emphasize that assemblages, such as staurolite + chloritoid + chlorite, should not be simply dismissed as disequilibrium occurrences without study,

3. Suggest the importance of determining the exact composition of the phases at which certain reactions, such as garnet + chlorite + muscovite = biotite + chloritoid + quartz + H_2O, proceed naturally. It may then be possible to reproduce this experimentally, using muscovite, quartz, and garnet and chlorite of the proper composition as reactants.

ACKNOWLEDGMENTS

I am indebted to Fred Barker and E-an Zen of the U. S. Geological Survey, W. G. Ernst of the University of California at Los Angeles, and L. S. Hollister, California Institute of Technology, for their critical comments on the manuscript. The work was supported by a grant from the National Science Foundation.

REFERENCES

Albee, A. L., 1952, Comparison of the chemical analyses of sedimentary and metamorphic rocks [abs.]: Geol. Soc. America Bull., v. 63, p. 1229.

———— in press, Phase equilibria in three assemblages of kyanite-zone pelitic schists, Lincoln Mountain quadrangle, central Vermont: Jour. Petrology, in press.

Aramaki, S., and Roy, R., 1963, A new polymorph of Al_2SiO_5 and further studies in the system Al_2O_3–SiO_2–H_2O: Am. Mineralogist, v. 48, p. 1322-1347.

Barker, Fred, 1962, Cordierite-garnet gneiss and associated microcline-rich pegmatite at Sturbridge, Massachusetts, and Union, Connecticut: Am. Mineralogist, v. 47, p. 907-918.

Bell, P. M., 1963, Aluminum silicate system: experimental determination of the triple point: Science, v. 139, p. 1055-1056.

Best, M. G., and Weiss, L. E., 1964, Mineralogical relations in some pelitic hornfels from the southern Sierra Nevada, California: Am. Mineralogist, v. 49, p. 1240-1266.

Chinner, G. A., 1962, Almandine in thermal aureoles: Jour. Petrology, v. 3, p. 316-340.

Clark, S. P., Jr., 1961, A redetermination of equilibrium relations between kyanite and sillimanite: Am. Jour. Sci., v. 259, p. 641-650.

Deer, W. A., Howie, R. A., and Zussman, J., 1962, Rock-forming minerals; v. 1, Ortho- and ring-silicates: London, Longmans, Green, and Co., Ltd., 333 p.

Francis, G. H., 1956, Facies boundaries in pelites at the middle grades of regional metamorphism: Geol. Mag., v. 93, p. 353-368.

Fyfe, W. S., Turner, F. J., and Verhoogan, John, 1958, Metamorphic reactions and metamorphic facies: Geol. Soc. America Mem. 73, 259 p.

Green, J. C., 1963, High-level metamorphism of pelitic rocks in northern New Hampshire: Am. Mineralogist, v. 48, p. 991-1023.

Greenwood, H. J., 1961, The system $NaAlSi_2O_6$–H_2O–Argon; total pressure and water pressure in metamorphism: Jour. Geophys. Research, v. 66, p. 3923-3946.
Halferdahl, L. B., 1961, Chloritoid; its composition, x-ray and optical properties, stability, and occurrence: Jour. Petrology, v. 2, p. 49-135.
Juurinen, A., 1956, Composition and properties of staurolite: Acad. Sci. Fennicae Annales, ser. A III, Geol.-Geog. 47, 53 p.
Kennedy, G. C., 1950, Pressure–volume–temperature relations in water at elevated temperatures and pressures: Am. Jour. Sci., v. 248, p. 540-564.
———— 1959, Phase relations in the system Al_2O–H_2O at high temperatures and pressures: Am. Jour. Sci., v. 257, p. 563-573.
Khitarov, N. I., Pugin, V. A., Chao, Pin, and Slutskii, A. B., 1963, Relation between andalusite, kyanite and sillimanite at moderate temperatures and pressures: Geochemistry (translation of Geokhimiia), v. 3, p. 325-244.
Korzhinskii, D. S., 1959, Physiocochemical basis of the analysis of the paragenesis of minerals: New York, Consultants Bureau, Inc., 143 p. (translated from the Russian).
Latimer, W. M., 1951, Methods of estimating the entropy of solid compounds: Am. Chem. Soc. Jour., v. 73, p. 1480-1482.
Miyashiro, Akiho, 1958, Regional metamorphism of the Gosaisyo-Takanuki district in the central Abukuma Plateau: Tokyo Univ. Fac. Sci. Jour., sec. 2, v. 11, p. 219-272.
———— 1961, Evolution of metamorphic belts: Jour. Petrology, v. 2, p. 277-311.
Niggli, P., 1954, Rocks and mineral deposits: San Francisco, W. H. Freeman and Co., 559 p.
Pankratz, L. B., 1964, High-temperature heat contents and entropies of muscovite and dehydrated muscovite: U. S. Bur. Mines Rept. Inv. 6371, 6 p.
Phinney, W. C., 1963, Phase equilibria in the metamorphic rocks of St. Paul Island and Cape North, Nova Scotia: Jour. Petrology, v. 4, p. 90-130.
Read, H. H., 1952, Metamorphism and migmatisation in the Ythan Valley, Aberdeenshire: Edinburgh Geol. Soc. Trans., v. 15, p. 265-279.
Roy, Rustum, and Osborn, E. F., 1954, The system Al_2O_3–SiO_2–H_2O: Am. Mineralogist, v. 39, p. 853-885.
Schreyer, W. F., and Schairer, J. F., 1961, Compositions and structural states of anhydrous Mg-cordierites; a re-investigation of the central part of the system MgO–Al_2O_3–SiO_2: Jour. Petrology, v. 2, p. 324-406.
Schreyer, W. F., and Yoder, H. S., Jr., 1964, The system Mg–cordierite–H_2O and related rocks: Neues Jahrb. Mineralogie Abh., v. 101, p. 271-342.
Segnit, R. E., and Kennedy, G. C., 1961, Reactions and melting relations in the system muscovite–quartz at high pressures: Am. Jour. Sci., v. 259, p. 280-287.
Shirozu, H., 1958, X-ray powder patterns and cell dimensions of some chlorites in Japan, with a note on their interference colors: Mineralog. Jour., v. 2, p. 209-223.
Skinner, B. J., 1956, Physical properties of end members of the garnet group: Am. Mineralogist, v. 41, p. 428-436.
Skinner, B. J., Clark, S. P., Jr., and Appleman, D. E., 1961, Molar volumes and thermal expansions of andalusite, kyanite, and sillimanite: Am. Jour. Sci., v. 259, p. 651-668.
Snelling, N. J., 1957a, A note on the composition of staurolite from the Caenlochan schists: Mineralog. Mag., v. 31, p. 603-604.
———— 1957b, A contribution to the mineralogy of chloritoid: Mineralog. Mag., v. 31, p. 469-475.
Thompson, J. B., Jr., 1955, The thermodynamic basis for the mineral facies concept: Am. Jour. Sci., v. 253, p. 65-103.
———— 1957, The graphical analysis of mineral assemblages in pelitic schists: Am. Mineralogist, v. 42, p. 842-858.
———— 1961, Mineral facies in pelitic schists (English summ.): Moscow, Akad. Nauk SSSR, Korzhinskii festschr, p. 313-325.
Troger, W. E., 1963, Der geothermische gradient im pt-Feld der metamorphen Facies: Beitr. Mineralogie und Petrographie, v. 9, p. 1-12.
Wones, D. R., 1963, Physical properties of synthetic biotites on the join phlogopite–annite: Am. Mineralogist, v. 48, p. 1300-1321.
Yoder, H. S., Jr., 1952, The MgO–Al_2O_3–SiO_2–H_2O system and the related metamorphic facies: Am. Jour. Sci., Bowen v., p. 569-627.
Yoder, H. S. Jr., and Eugster, H. P., 1955, Synthetic and natural muscovites: Geochim. et Cosmochim. Acta, v. 8, p. 225-280.